Science Arts & Métiers (SAM)

is an open access repository that collects the work of Arts et Métiers Institute of Technology researchers and makes it freely available over the web where possible.

This is an author-deposited version published in: https://sam.ensam.eu
Handle ID: .http://hdl.handle.net/10985/15177

To cite this version :

Faissal CHEGDANI, Mohamed EL MANSORI, Sabeur MEZGHANI, Alex MONTAGNE - Scale effect on tribo-mechanical behavior of vegetal fibers in reinforced bio-composite materials - Composites Science and Technology - Vol. 150, p.87-94 - 2017

Any correspondence concerning this service should be sent to the repository Administrator : archiveouverte@ensam.eu

Arts et Métiers Institute of Technology

Composites Science and Technology

Scale effect on tribo-mechanical behavior of vegetal fibers in reinforced bio-composite materials

Faissal Chegdani*, Mohamed El Mansori, Sabeur Mezghani, Alex Montagne

Arts et Métiers ParisTech, MSMP / EA7350, Rue Saint Dominique, BP 508, 51006 Châlons-en-Champagne, Cedex, France

Keywords:
Vegetal fibers
Polymer-matrix composites (PMCs)
Friction/wear
Mechanical properties
Atomic force microscopy (AFM)

A B S T R A C T

The nature of friction of vegetal fiber and polymeric matrix in bio-composite materials is very important for many industrial applications. In order to design natural fiber composites for structural applications, the scientific understanding of tribo-mechanical phenomena inside the heterogeneous structure of natural fibers and also the overall heterogeneous structure of the bio-composite is required. This implies a special focus on the fundamental aspects of vegetal fiber friction at the macro-, meso-, and microscale. This research paper investigates the multiscale mechanical and friction properties of natural fibers. The mechanical properties of flax fibers, glass fibers (as a reference) and polypropylene matrix has been evaluated at microscale and mesoscale by Atomic Force Microscopy (AFM) and Nanoindenter XP (MTS Nano Instruments), respectively, using nanoindentation technique. At the macroscale, the mechanical behavior has been considered for the global composite structure. The micro-friction response of each composite component has been measured by instrumenting AFM for scratch test technique. The results show the scale dependence of mechanical behavior for flax fibers, unlike glass fibers and polypropylene matrix where their mechanical performances are independent of the analysis scale. Tribological results in terms of dynamic friction coefficient show that flax fibers induce more friction than glass fibers, while polypropylene matrix generates the highest friction. This is sign that vegetal fiber friction is scale dependent property as shown when referring to the contact mechanics theory. The arisen results are very important for many technical applications in PMCs surface engineering based on plant fibers.

1. Introduction

The industrial world is becoming more and more interested in bio-materials due to the many economic and environmental requirements [1–5]. Bio-based materials have different designations such as “green”, “biodegradable” or “eco-friendly” materials. In fact, this label is broad, but it generally refers to one of two scenarios: materials that incorporate a biological material or materials in which one or more components are derived from natural materials [6]. A primary example of the first category is natural fiber reinforced polymer composites, which are the aim of this work. The polymer matrices themselves may be either petrochemical or natural in origin [6].

The bio-composites are increasingly demanded by automotive and aerospace industries, especially the vegetal fiber composites thanks to the high mechanical properties of plant fibers [7,8]. However, the complex structure of vegetal fibers makes difficult the understanding of their mechanical and tribological behaviors [6,9]. This prevents a good control of their manufacturing processes, typically in machining process where it was shown in previous work of the authors that the behavior of plant fibers during the cutting operations differs according to the scale chosen for the analysis [10–13]. This is induced by the multiscale structure of the fibrous reinforcement where the vegetal elementary fibers are gathered in bundles and each elementary fiber is itself a composite of cellulosic microfibrils in a natural matrix of hemicellulose and lignin [6,9]. These specific structure and composition of vegetal fibers influence the mechanical and tribological behavior of the fibrous reinforcement inside the composite under the machining operations. For all these reasons, it is important to conduct a multiscale characterization of both mechanical and tribological behavior of vegetal fibrous reinforcements in order to understand their cutting behavior.

The nanoindentation technique is an efficient method to reveal the mechanical properties of many materials in terms of stiffness,

* Corresponding author.
E-mail address: faissal.chegdani@ensam.eu (F. Chegdani).

especially for fibrous materials where the contact area is very small. Some nanoindentation work have been conducted on glass fibers using Atomic Force Microscopy (AFM) [14,15], tribo-indenter [16], AFM adapted with commercial nanoindenter [17] or instrumented indentation (IIT) [14]. All these work reveal a homogeneous behavior of glass fibers with an elastic Young modulus between 60 GPa and 90 GPa depending on the type of the glass fibers used in each of these studies which correspond to the standard elastic modulus of glass fibers obtained by tensile tests [1,4]. Vegetal fibers have also been characterized with a commercial nanoindentation instrument (Nanoindenter XP, MTS Nano Instruments) for different fiber types [18–21]. With this nanoindentation technique, the elastic modulus is around 18 GPa for flax fibers and 12 GPa for hemp fibers [19] which is lower than the standard values obtained by tensile tests [1,4]. It may be due to the heterogeneity of vegetal fibers and this issue requires a rigorous characterization of vegetal fiber behavior at different contact scales.

In this paper, two composite materials were considered. The first is representative of the engineering structure of bio-based composites (flax fiber + PP matrix). The second is representative of the engineering structure of synthetic composites commonly used in automotive and aerospace industry (glass fibers + epoxy matrix). This study will focus on the local mechanical and tribological responses of flax fibers, glass fibers and PP matrix separately to isolate their tribo-mechanical effects within their own composite structure.

The analysis of tribo-mechanical properties is essentially based on the contact area between the indenter tip and the material surface, which defines the contact scale. AFM and Nanoindenter XP (MTS Nano Instruments) have been used to generate different contact scales. The first part of this research paper consists on nanoindentation tests to reveal the elastic properties of flax fibers, glass fibers and PP matrix depending on the indentation contact scale. The second part relies to micro-scratch test experiments in order to determine the local friction response inside each composite material component.

2. Experimental procedure

2.1. Material

Glass fibers, flax fibers and PP matrix are indented inside composites workpieces in order to facilitate the experimental setup. Flax fibers and PP matrix are commingled together in one composite material supplied by "*Composites Evolution - UK*" (Fig. 1(b)). As a reference material, glass fibers are investigated from composite workpieces of glass fibers and epoxy resin that are elaborated by thermocompression of prepreg sheets (Fig. 1(a)). The epoxy matrix is not considered in this study. In the two workpieces, the fibrous reinforcement is unidirectional and the fibers are perpendicular to the worksurface in order to work on the cross section of the fibers. All the worksurfaces have been polished with the same grit size (~5 μm) of sand paper in order to have the same initial surface state before characterizations.

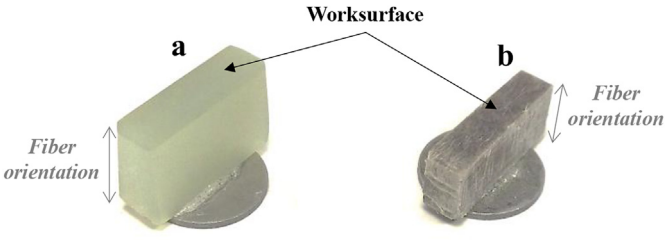

Fig. 1. a) glass/epoxy workpiece. b) flax/PP workpiece.

2.2. Nanoindentation tests

Nanoindentation tests have been conducted using two different tools. The atomic force microscopy (AFM) instrument "*Dimension Edge™ - Bruker*" has been used with a Berkovich diamond tip indenter at small tip radius (~40 nm). The tip indenter is related to a steel cantilever that has a spring constant of 450 N/m.

The commercial nanoindentation instrument "*Nanoindenter XP/ MTS Nano Instruments*" has been used with a Berkovich diamond tip indenter at high tip radius (~400 nm). The tip indenter is related to a mobile column that can move vertically.

Nanoindentation tests involve the contact of an indenter on a material surface and its penetration of the surface to a specified load or depth [19]. Load is measured as a function of penetration depth as shown in Fig. 2. From this load–penetration curve, the pertinent parameters for the analysis are the maximum displacement (h_{max}), the maximum load on the sample (F_{max}) and the contact stiffness (S), which is the slope of the tangent line to the unloading curve at the maximum loading point (see Fig. 2).

It's important to note that a calibration step is done before indentation on the studied workpieces. For AFM instrument, the calibration step consists on making indentation tests on very hard material (tungsten carbide in this case) with low loading in order to determine the cantilever displacement without penetration of the tip indenter into the worksurface. This own displacement of the cantilever is then reduced from the global measured displacement when indenting the studied workpieces in order to determine the real penetration depth (h_{max}).

For MTS instrument, the moving column deforms during indentation. This phenomenon is called "machine complacency". The supplier calibrates it once and for all. The data displayed by the instrument are already adjusted for this complacency.

In the case of Berkovich tip indenter, the model of Oliver & Pharr [22] is suitable to calculate the elastic modulus of each material using the parameters extracted from load–penetration curve of Fig. 2. The Oliver & Pharr method consists on computing the contact depth (h_c), which is dependent on the material deformation and the tip shape as shown in Fig. 3 h_c can be calculated using Eq (1). ε is a constant related to the tip geometry (0.72 for Berkovich tip [19]). The projected contact area (A) can be calculated using Eq (2). Then, the reduced elastic modulus is obtained by Eq (3) where β is a

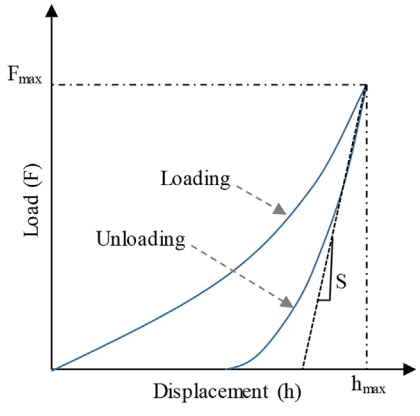

Fig. 2. Typical indentation curve showing the pertinent parameters for elastic modulus calculation.

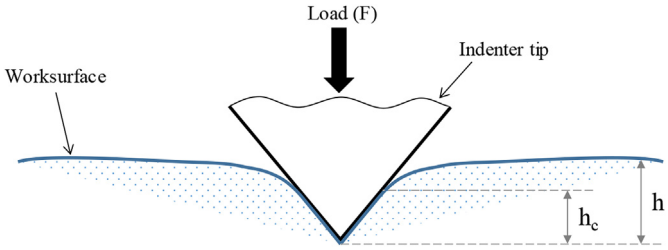

Fig. 3. Schematization of indentation process showing the penetration parameters.

constant related to the tip geometry (1.034 for Berkovich tip [19]). Finally, the elastic modulus of the indented material can be calculated via Eq (4) where E_i and ν_i are the elastic modulus and the Poisson coefficient of the tip indenter ($E_i = 1140$ GPa and $\nu_i = 0.07$ for diamond tip). ν is the Poisson coefficient of the indented material. It's important to notice that both Doerner & Nix [23] followed by Oliver & Pharr [22], have assumed elastic behavior as the basis foundation of this calculation procedure.

$$h_c = h_{max} - \varepsilon \frac{F_{max}}{S} \tag{1}$$

$$A = 24.56 \times {h_c}^2 \tag{2}$$

$$E_r = \frac{S\sqrt{\pi}}{2\beta\sqrt{A}} \tag{3}$$

$$\frac{1}{E_r} = \frac{(1-\nu^2)}{E} + \frac{(1-{\nu_i}^2)}{E_i} \tag{4}$$

2.3. Scratch tests

Tribological scratch tests have been made by AFM. The tip indenter slides on the worksurface at constant load and sliding speed. The target sliding distance is 10 μm in order to work separately on the elementary fiber zone or the polymer matrix zone. The friction signal is measured over the sliding distance and the dynamic friction coefficient is determined by computing the ratio between the mean friction signal and the applied load at each sliding condition. Table 1 presents the studied sliding conditions.

Table 1
Sliding conditions for AFM scratch tests.

Applied load (μN)	Sliding speed (μm/s)
10	2
20	4
30	6
	8
	10

3. Results and discussion

3.1. Multiscale mechanical properties

3.1.1. AFM nanoindentation

AFM instrument has been used in tapping mode for nanoindentation tests. The considered zone for the indentations (50 μm × 50 μm) has been scanned by the same AFM mode in order to well target the tip indenter position at each indentation. Fig. 4 shows the scanned surface of the workpieces before indentation. These scan images reveal the difference between the flax fibers and the glass fibers in terms of shape, size and fiber distributions because flax fibers have heterogeneous polygonal shapes and are gathered in bundles, while glass fibers have homogenous cylindrical shapes and are well separated.

In order to have comparable measurements for all the studied materials, all indentations have been realized at a maximum load of $F_{max} = 500$ μN. Fig. 5 shows the work zones after indentation. The Berkovich indentation traces can be clearly seen on flax fibers and PP matrix. However, the indentations traces are less observed in glass fibers. Indeed, at iso-loading, the indentation depths are not the same between glass and flax fibers. The behavior of flax fibers seems to be the same as the behavior of PP matrix at this scale of indentation contact. This finding is confirmed by a comparison between unloading indentations curves of the three studied materials (Fig. 6). The stiffness of glass fibers is higher than that of flax fibers at microscales. Moreover, flax fibers seem to behave like PP matrix with more penetration depth for flax fibers.

Fig. 7 presents the elastic modulus obtained for the three studied materials regarding the contact depth (h_c). Globally, the elastic modulus decreases by contact depth increasing. For glass fibers (Fig. 7(a)), elastic modulus is between 90 GPa and 95 GPa for low values of contact depth (between 17.5 nm and 19.5 nm) as it was observed on indentation traces of Fig. 5(c). Elastic modulus of PP (Fig. 7(b)) matrix is between 1 GPa and 2 GPa for more important contact depth comparing to glass fibers (between 70 nm and

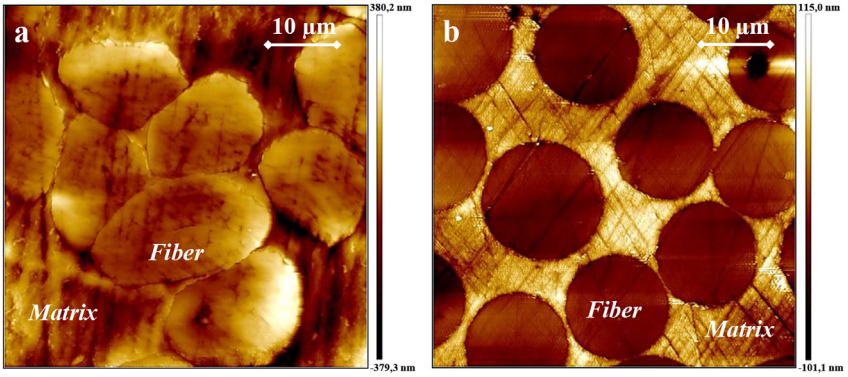

Fig. 4. Topographic AFM images before indentation for (a) flax/PP and (b) glass/epoxy.

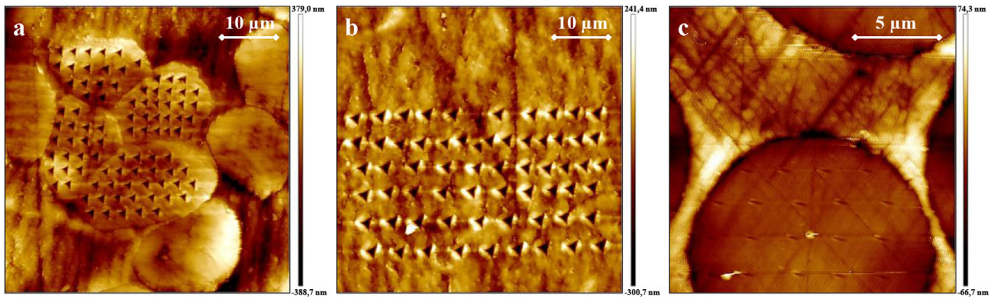

Fig. 5. Topographic AFM images after indentations for (a) flax fibers (b) PP matrix and (c) glass fiber.

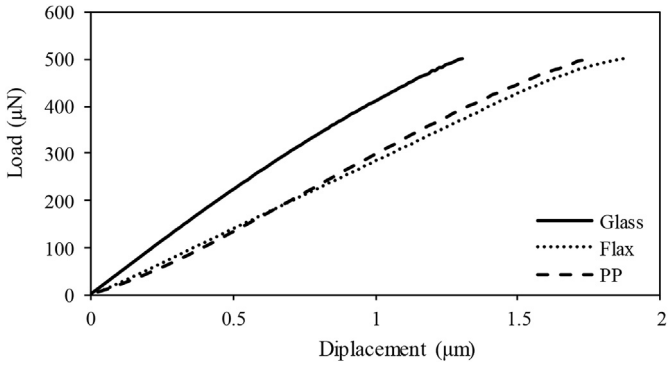

Fig. 6. Unloading curves obtained by AFM indentation for the studied materials.

150 nm). Flax fibers (Fig. 7(c)) show the lowest elastic modulus (between 0.65 GPa and 1 GPa) for contact depths greater than that of PP matrix (between 170 nm and 210 nm).

3.1.2. MTS nanoindentation

The objective of realizing nanoindentation tests with MTS nanoindenter is to increase the contact scale between the tip indenter and material surface. Fig. 5(a) shows that the AFM indentation trace size is about 1 µm on flax fibers. Fig. 8 presents the MTS indentation trace size on the same material (flax/PP). It can be seen that the MTS indentation trace size is greatly higher than that of AFM (~20 µm) and it solicits at least all the cross section of one elementary fiber since the flax fiber diameter is between 10 µm and 20 µm. Then, MTS indenter solicits the flax fibers on mesoscopic scale of the technical fibers (i.e fibers bundle) while AFM indenter solicits the flax fibers on microscopic scale of an elementary fiber.

MTS nanoindentation test has been performed with a continuous stiffness measurement (CSM) technique. In this technique, an oscillating force at controlled frequency and amplitude is superimposed onto a nominal applied force. The material, which is in contact with the oscillating force, responds with a displacement phase and amplitude. MTS nanoindentation instrument allows access to contact depths that cannot be achieved by AFM.

Fig. 9 illustrates the elastic modulus results regarding the contact depth (h_c). It can be seen that the three materials generate the same behavior. Indeed, the elastic modulus of each material is at its maximum at the beginning of loading for the low contact depth. Drastic decreasing of modulus is observed when increasing the contact depth. The elastic modulus becomes quasi constant from certain value of contact depth (~100 µm). However, glass fibers are the most sensitive to the variation of contact depth (Fig. 9(a)).

With MTS nanoindentation, for a contact depth range between 0 and 500 nm, glass fibers have an elastic modulus between 60 GPa and 95 GPa (Fig. 9(a)), PP matrix has an elastic modulus between

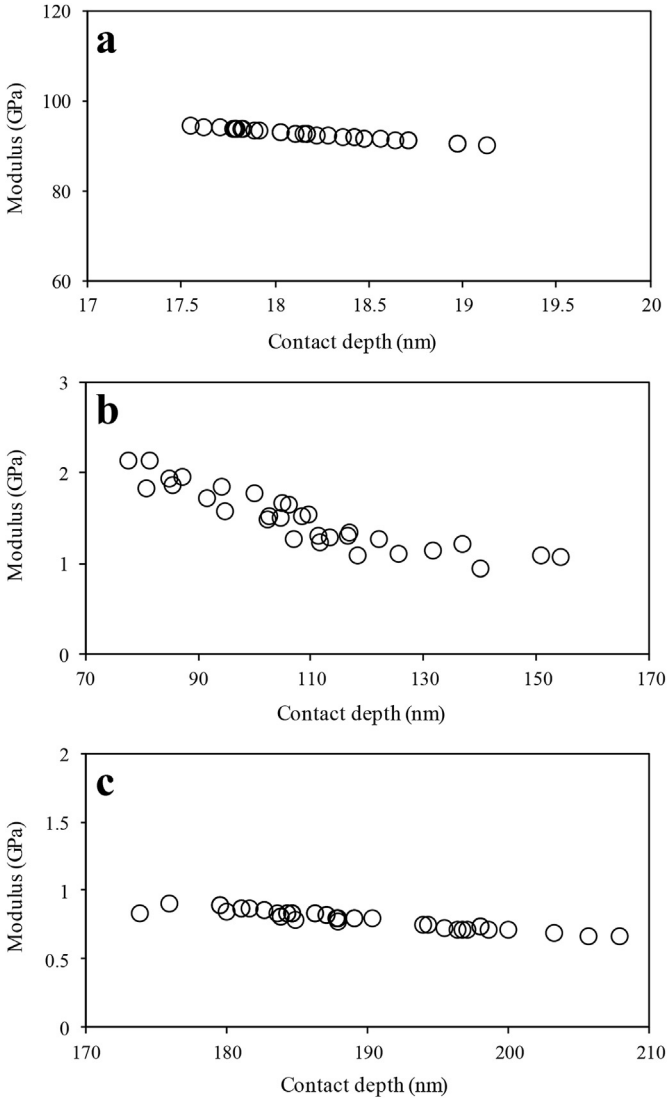

Fig. 7. Elastic modulus obtained by AFM indentation for (a) glass fibers, (b) PP matrix and (c) flax fibers.

2 GPa and 5 GPa (Fig. 9(b)) and flax fibers have an elastic modulus between 11 GPa and 22 GPa (Fig. 9(c)). It's important to notice in the three graphs of Fig. 9 that the variation of elastic modulus of both glass fibers and PP matrix is essentially due to contact depth variation. In the case of flax fibers, the elastic modulus variation is particularly due to the dispersion of the different fibers selected for the measurements.

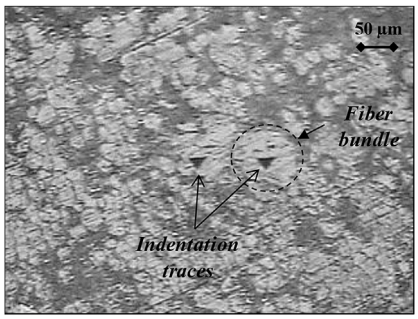

Fig. 8. Optical image showing indentation traces on flax fibers by MTS instrument.

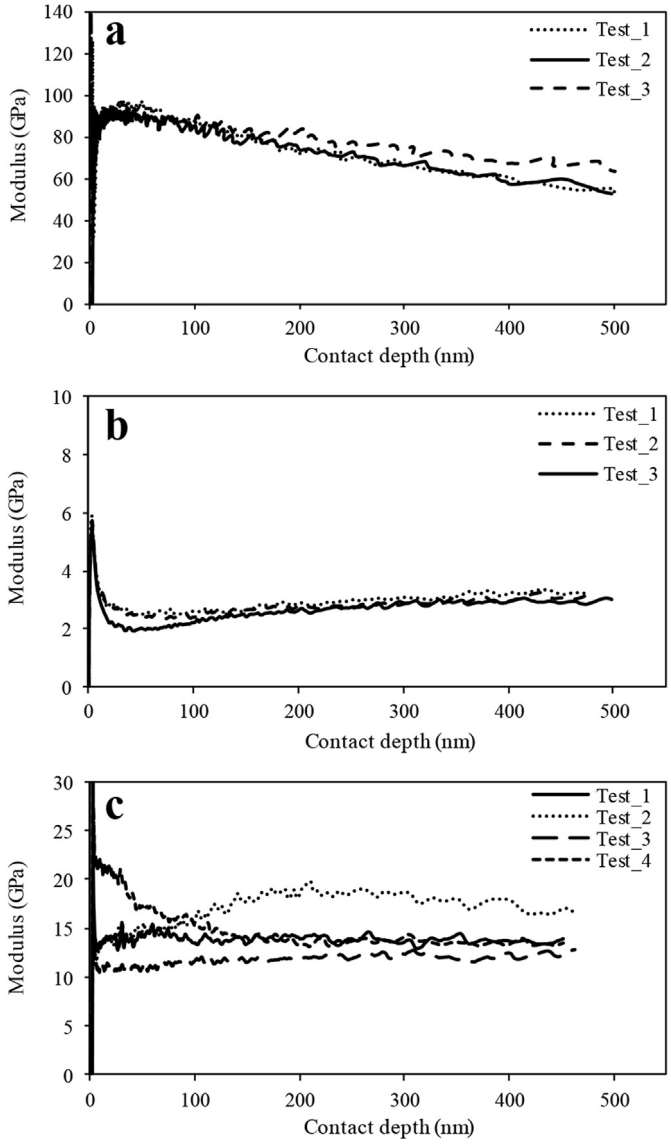

Fig. 9. Elastic modulus obtained by MTS indentation for (a) glass fibers, (b) PP matrix and (c) flax fibers.

3.2. Multiscale comparison of mechanical properties

To compare the mechanical properties of vegetal fiber composites on the different characteristic scales (micro-, meso- and macroscale), AFM and MTS results were compared on the same graph by only taking into account the contact depths range generated by the AFM nanoindentation. This allows the comparison the mechanical properties at microscale by AFM indentation, at mesoscale by MTS indentation and at macroscale from literature values with tensile tests [1,4].

Fig. 10(a) illustrates the multiscale comparison of elastic modulus for glass fibers. AFM and MTS indentations generate similar values at microscales and mesoscales, respectively. These values are slightly higher than those of tensile test at macroscales because displacements and deformations are more important in the case of tensile tests, which can reduce the stiffness by the contribution of the plastic component. Indeed, the literature values can be reached by increasing the contact depth as shown in Fig. 9(a). Generally, the modulus values are in the same order of magnitude for the three characteristic contact scales.

Fig. 10(b) presents the same comparison for PP matrix. As for the glass fibers, the modulus obtained by nanoindentation is slightly higher than the one from the literature. The AFM modulus decreases with the contact depth to become similar to the one of the literature. The modulus values are also on the same order of magnitude.

However, flax fibers exhibit different behavior. Fig. 10(c) shows the important variation of the modulus values when changing the contact scale for the mechanical characterization. Unlike glass fibers and PP matrix, the values of modulus obtained by nanoindentation are lower than those reported in the literature. There is a considerable difference between the elastic modulus values according to the contact scale. Indeed, at micro-scale, the modulus values obtained by AFM nano-indentation are too low compared to those of literature (maximum of 1 GPa). The elastic modulus increases by increasing the scale of contact. Thus, at meso-scale, the modulus values obtained by MTS nanoindenter are higher than AFM values but still lower than those obtained at macro-scale from the literature. There can also be notice an increase of the scatter by increasing the contact scale.

To synthesize this experimental comparative analysis, Fig. 11 presents the modulus values for the three materials at the different characteristic contact scales. It is clear that flax fibers are the most impacted by changing the contact scale during the mechanical characterization. The elastic modulus for the flax fibers, and unlike glass fibers, significantly increases by increasing the contact scale. This is mainly due to the specific heterogeneous structure of vegetal fiber. Indeed, vegetal fiber is itself a composite structure of cellulose microfibrils embedded in natural amorphous matrix of hemicellulose and lignin [9]. At microscale contact and with a tip radius of 40 nm, it is rather the natural polymer phase of the elementary fiber that is solicited at the indentation. Consequently, the resulted modulus values are approximately those of the polymers constituting the amorphous phase of elementary flax fibers. By increasing the contact scale and the tip radius, the cellulose microfibrils, which control the stiffness of plant fibers, start to be solicited. Thus, the modulus of elasticity increases at meso-contact-scale. At macro-scale, all the cellulose microfibrils of elementary fibers are completely solicited and the elastic modulus becomes more important. The scatter of elastic modulus measurements increases considerably by increasing the scale of analysis in the case of flax fibers because the highest scales take much

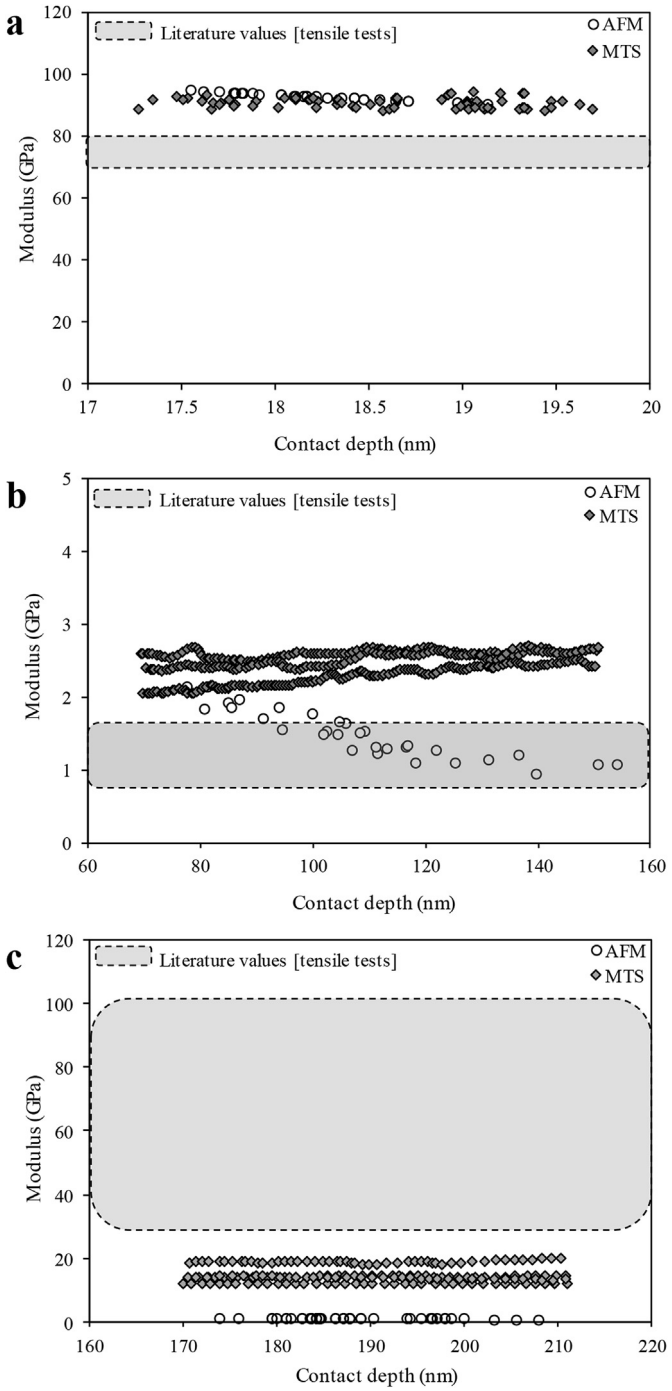

Fig. 10. Comparison of the elastic modulus obtained by AFM and MTS Nanoindenter with the literature results. (a) glass fiber, (b) PP matrix and (c) flax fibers.

more into account the random natural character of plant fibers (fibers shape, fibers size, microfibrils rate in elementary fiber, etc.).

3.3. Micro-friction properties

As for indentation tests, the worksurface zone has been scanned in order to choose the sliding distance on fibers only and polymer matrix only. AFM instrument is used in contact mode for the scratch tests. Fig. 12 illustrates the results of the dynamic friction coefficient (μ_D) at the different sliding conditions. The dynamic friction coefficient of glass fibers shows no significant dependence of sliding

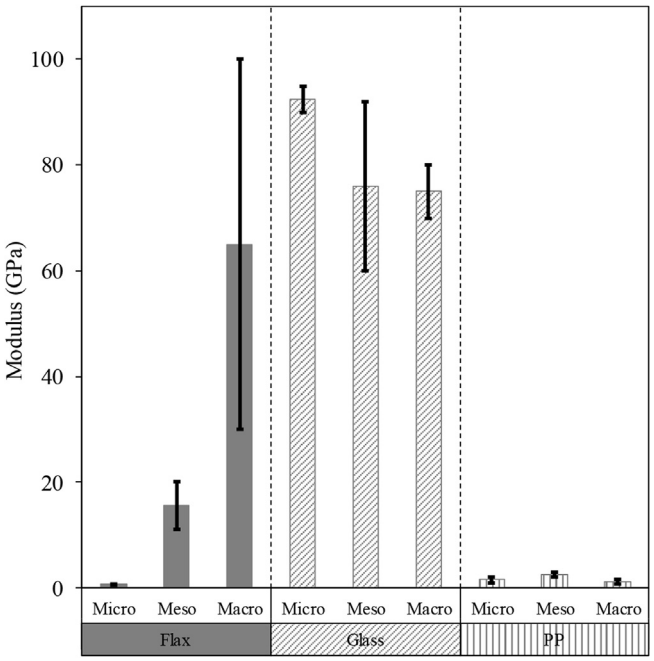

Fig. 11. Multiscale comparison of elastic modulus between flax fibers, glass fibers and PP matrix.

speed. However, the dynamic friction coefficient decreases significantly by increasing the applied load (Fig. 12(a)). For PP matrix, the dynamic friction coefficient slightly increases by sliding speed increasing and shows no significant dependence of the applied load (Fig. 12(b)). Flax fibers show a different tribological behavior. Indeed, there is an interaction between the effects of both sliding speed and applied load (Fig. 12(c)). The effect of sliding is hence observed at high applied load where increasing the sliding speed decreases the dynamic friction coefficient. This effect disappears at low applied load. On the other side, the effect of the applied load is conspicuous at low sliding speeds where increasing the applied load increases the dynamic friction coefficient, unlike the glass fibers. Increasing the sliding speed inhibits the effect of the applied load.

At this micro-tribo-contact scales (i.e. AFM contact scales), glass fibers show the same tribological behavior as at the macro-tribo-contact scales at dry conditions where the dynamic friction coefficient decreases also by increasing the applied load and sliding speed [24] except that, at micro-tribo-contact scales, there is no influence of sliding speed and this can be due to the low sliding distance at this contact scales.

Flax fibers show tribological behavior opposed to glass fibers at micro-contact scales where the dynamic friction coefficient decreases by increasing the applied load. Indeed, even if the scratch tests have been performed at dry conditions, vegetal fibers are a hydrophilic material and have high ability to absorb humidity. Vegetal fibers can absorb a large amount of water flow into their fiber cell wall due to the fact that cellulose, lignin and hemicelluloses possess polar hydroxyl groups which are highly attractive to the hydrogen bonds of water present in humid environment [25]. Consequently, and locally at the contact scale, the hydrophilicity of the vegetal fiber modifies the contact interface by the presence of thin film of water. Then, it changes the real contact surface by activating capillarity effects. This phenomenon makes flax fibers have the same macro-tribological behavior as glass fibers at water-lubricated contact where the dynamic friction coefficient increases by applied load increasing [24].

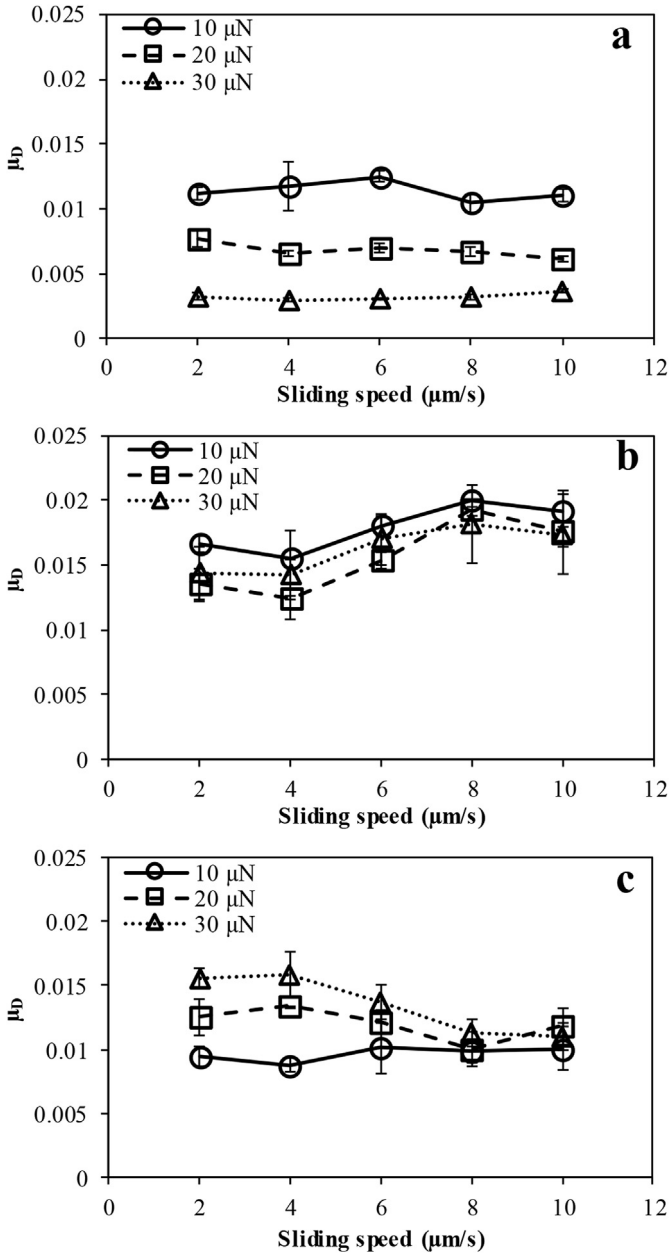

Fig. 12. Dynamic friction coefficient obtained by AFM scratch test for different applied loads. (a) glass fibers, (b) PP matrix and (c) flax fibers.

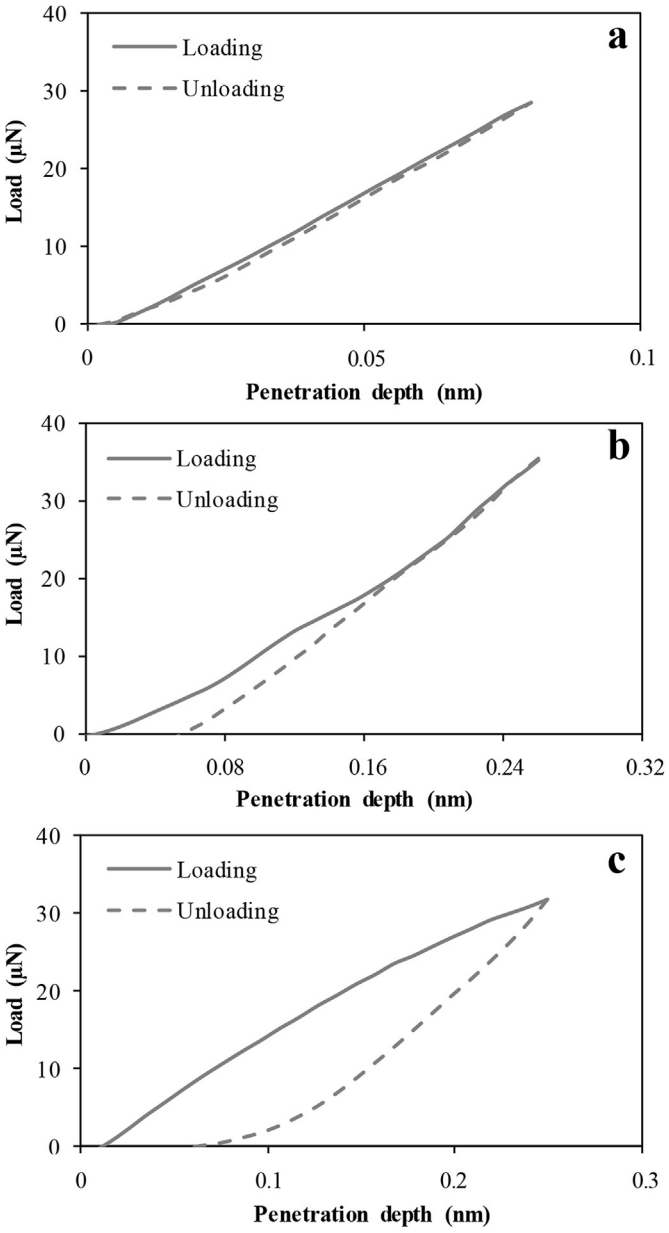

Fig. 13. Typical mechanical curves obtained by AFM indentation. (a) glass fibers, (b) PP matrix and (c) flax fibers.

By comparing the dynamic friction coefficient values, it can be seen that, surprisingly, the dynamic friction coefficient of flax fibers is higher than that of glass fibers. It's well known at macroscales that glass fibers generate higher friction than flax fibers due to the abrasive character of glass fibers [26–28]. PP matrix generates the highest dynamic friction coefficient and it's coherent with the tribological behavior of polymers at macroscales where the dynamic friction coefficient increased by the contribution of adhesion and deformation mechanisms [29,30].

The micro-tribological behavior can be explained locally by the micromechanical behavior of each material when the contact with the tip indenter. To understand the mechanical difference between the three-studied materials, Fig. 13 shows the nanoindentation curves obtained by AFM. It can be seen that, at iso-loading, glass fibers generate an elastic behavior, PP matrix have a plastic behavior while flax fibers exhibit a viscoelastic behavior. It's well known that heterogeneous viscoelastic behavior increases the dynamic friction coefficient by adding a supplementary component [31]. The same contribution of the plastic component can increase the dynamic friction coefficient [32]. These contributions of mechanical components on tribological behavior can explain the highest dynamic friction coefficient of flax fiber and PP matrix regarding the glass fibers.

4. Conclusions

The multiscale tribo-mechanical behaviors of flax fibers, glass fibers and polypropylene matrix have been investigated in this paper. Multiscale mechanical and tribological analyses have been conducted using respectively nanoindentation and scratch tests. AFM and MTS nanoindenter instruments have been used to perform work-surface characterizations as function of the target

scale analysis. The following conclusions can be drawn:

- The elastic modulus of flax fibers obeys the law of scale effect. The fiber stiffness increases significantly when the contact scale increasing. This is due to the heterogeneity of the vegetal fibrous reinforcement where increasing the contact scale will increase the cellulose microfibrils rate into contact that control the fiber stiffness.
- Glass fibers and PP matrix, which are homogenous materials, don't show a significant variation of elastic modulus by increasing the analysis scale.
- Flax fibers generate more friction than glass fibers while PP matrix shows the highest friction coefficient. This result is related to the mechanical behavior of each material at the same scale. The viscoelastic behavior of flax fibers and the plastic behavior of PP matrix add a supplementary component to the dynamic friction coefficient. This finding must be considered when designing bio-composites for tribological applications.
- Flax fibers and glass fibers don't behave in the same way in terms of friction trend. The dynamic friction coefficient of glass fibers decreases by load increasing while the apparent friction of flax fibers increases by load increasing. The special tribological behavior of flax fiber can be due to the hydrophilic character of vegetal fibers, which contain water molecules. This induces a specific tribological contact like water-lubricated contact.

Acknowledgments

The authors acknowledge the urban community of *Châlons-en-Champagne* (*Cités-en-Champagne*) for the financial support.

References

[1] D.B. Dittenber, H.V.S. GangaRao, Critical review of recent publications on use of natural composites in infrastructure, Compos. Part A Appl. Sci. Manuf. 43 (2012) 1419–1429, http://dx.doi.org/10.1016/j.compositesa.2011.11.019.
[2] O. Faruk, A.K. Bledzki, H.-P. Fink, M. Sain, Biocomposites reinforced with natural fibers: 2000–2010, Prog. Polym. Sci. 37 (2012) 1552–1596, http://dx.doi.org/10.1016/j.progpolymsci.2012.04.003.
[3] M. John, S. Thomas, Biofibres and biocomposites, Carbohydr. Polym. 71 (2008) 343–364, http://dx.doi.org/10.1016/j.carbpol.2007.05.040.
[4] D.U. Shah, Developing plant fibre composites for structural applications by optimising composite parameters: a critical review, J. Mater. Sci. 48 (2013) 6083–6107, http://dx.doi.org/10.1007/s10853-013-7458-7.
[5] P. Wambua, J. Ivens, I. Verpoest, Natural fibres: can they replace glass in fibre reinforced plastics? Compos. Sci. Technol. 63 (2003) 1259–1264, http://dx.doi.org/10.1016/S0266-3538(03)00096-4.
[6] W. Brostow, H.E. Hagg Lobland, Materials: Introduction and Applications, John Wiley & Sons, Inc., New York, 2017. http://eu.wiley.com/WileyCDA/WileyTitle/productCd-0470523794.html (Accessed July 7, 2017).
[7] A. Shalwan, B.F. Yousif, In state of art: mechanical and tribological behaviour of polymeric composites based on natural fibres, Mater. Des. 48 (2013) 14–24, http://dx.doi.org/10.1016/j.matdes.2012.07.014.
[8] A. Lefeuvre, A. Bourmaud, C. Morvan, C. Baley, Tensile properties of elementary fibres of flax and glass: analysis of reproducibility and scattering, Mater. Lett. 130 (2014) 289–291, http://dx.doi.org/10.1016/j.matlet.2014.05.115.
[9] C. Baley, Analysis of the flax fibres tensile behaviour and analysis of the tensile stiffness increase, Compos. - Part A Appl. Sci. Manuf. 33 (2002) 939–948, http://dx.doi.org/10.1016/S1359-835X(02)00040-4.
[10] F. Chegdani, S. Mezghani, M. El Mansori, Correlation between mechanical scales and analysis scales of topographic signals under milling process of natural fibre composites, J. Compos. Mater. (2016), http://dx.doi.org/10.1177/0021998316676625.
[11] F. Chegdani, S. Mezghani, M. El Mansori, A. Mkaddem, Fiber type effect on tribological behavior when cutting natural fiber reinforced plastics, Wear 332–333 (2015) 772–779, http://dx.doi.org/10.1016/j.wear.2014.12.039.
[12] F. Chegdani, S. Mezghani, M. El Mansori, Experimental study of coated tools effects in dry cutting of natural fiber reinforced plastics, Surf. Coatings Technol. 284 (2015) 264–272, http://dx.doi.org/10.1016/j.surfcoat.2015.06.083.
[13] F. Chegdani, S. Mezghani, M. El Mansori, On the multiscale tribological signatures of the tool helix angle in profile milling of woven flax fiber composites, Tribol. Int. 100 (2016) 132–140, http://dx.doi.org/10.1016/j.triboint.2015.12.014.
[14] M.A. Monclus, T.J. Young, D. Di Maio, AFM indentation method used for elastic modulus characterization of interfaces and thin layers, J. Mater. Sci. 45 (2010) 3190–3197, http://dx.doi.org/10.1007/s10853-010-4326-6.
[15] T.J. Young, L.E. Crocker, W.R. Broughton, S.L. Ogin, P.A. Smith, Observations on interphase characterisation in polymer composites by nano-scale indentation using AFM and FEA, Compos. Part A Appl. Sci. Manuf. 50 (2013) 39–43, http://dx.doi.org/10.1016/j.compositesa.2013.03.014.
[16] N. Lonnroth, C.L. Muhlstein, C. Pantano, Y. Yue, Nanoindentation of glass wool fibers, J. Non. Cryst. Solids 354 (2008) 3887–3895, http://dx.doi.org/10.1016/j.jnoncrysol.2008.04.014.
[17] S.K. Khanna, P. Ranganathan, S.B. Yedla, R.M. Winter, K. Paruchuri, Investigation of nanomechanical properties of the interphase in a glass fiber reinforced polyester composite using nanoindentation, J. Eng. Mater. Technol. 125 (2003) 90, http://dx.doi.org/10.1115/1.1543966.
[18] A. Bourmaud, C. Baley, Rigidity analysis of polypropylene/vegetal fibre composites after recycling, Polym. Degrad. Stab. 94 (2009) 297–305, http://dx.doi.org/10.1016/j.polymdegradstab.2008.12.010.
[19] A. Bourmaud, S. Pimbert, Investigations on mechanical properties of poly(-propylene) and poly(lactic acid) reinforced by miscanthus fibers, Compos. Part A Appl. Sci. Manuf. 39 (2008) 1444–1454, http://dx.doi.org/10.1016/j.compositesa.2008.05.023.
[20] A. Bourmaud, C. Baley, Nanoindentation contribution to mechanical characterization of vegetal fibers, Compos. Part B Eng. 43 (2012) 2861–2866, http://dx.doi.org/10.1016/j.compositesb.2012.04.050.
[21] A. Le Duigou, A. Bourmaud, C. Baley, In-situ evaluation of flax fibre degradation during water ageing, Ind. Crops Prod. 70 (2015) 204–210, http://dx.doi.org/10.1016/j.indcrop.2015.03.049.
[22] W.C. Oliver, G.M. Pharr, An improved technique for determining hardness and elastic-modulus using load and displacement sensing indentation experiments, J. Mater. Res. 7 (1992) 1564–1583, http://dx.doi.org/10.1557/.
[23] M.F. Doerner, W.D. Nix, A method for interpreting the data from depth-sensing indentation instruments, J. Mater. Res. 1 (1986) 601–609. https://doi.org/10.1557/JMR.1986.0601.
[24] N.S. El-Tayeb, R.M. Gadelrab, Friction and wear properties of E-glass fiber reinforced epoxy composites under different sliding contact conditions, Wear 192 (1996) 112–117, http://dx.doi.org/10.1016/0043-1648(95)06770-1.
[25] B.F. Yousif, U. Nirmal, Wear and frictional performance of polymeric composites aged in various solutions, Wear 272 (2011) 97–104, http://dx.doi.org/10.1016/j.wear.2011.07.006.
[26] U. Nirmal, K.O. Low, J. Hashim, On the effect of abrasiveness to process equipment using betelnut and glass fibres reinforced polyester composites, Wear 290–291 (2012) 32–40, http://dx.doi.org/10.1016/j.wear.2012.05.022.
[27] B.F. Yousif, N.S.M. El-Tayeb, Adhesive wear performance of t-OPRP and UT-OPRP composites, Tribol. Lett. 32 (2008) 199–208, http://dx.doi.org/10.1007/s11249-008-9381-7.
[28] U. Nirmal, J. Hashim, K.O. Low, Adhesive wear and frictional performance of bamboo fibres reinforced epoxy composite, Tribol. Int. 47 (2012) 122–133, http://dx.doi.org/10.1016/j.triboint.2011.10.012.
[29] W. Brostow, V. Kovacevic, D. Vrsaljko, J. Whitworth, Tribology of polymers and polymer-based composites, J. Mater. Educ. 32 (2010) 273–290.
[30] N.K. Myshkin, M.I. Petrokovets, A.V. Kovalev, Tribology of polymers: adhesion, friction, wear, and mass-transfer, Tribol. Int. 38 (2005) 910–921, http://dx.doi.org/10.1016/j.triboint.2005.07.016.
[31] K.E. Koumi, T. Chaise, D. Nelias, Rolling contact of a rigid sphere/sliding of a spherical indenter upon a viscoelastic half-space containing an ellipsoidal inhomogeneity, J. Mech. Phys. Solids 80 (2015) 1–25, http://dx.doi.org/10.1016/j.jmps.2015.04.001.
[32] J. Bucaille, E. Felder, G. Hochstetter, Mechanical analysis of the scratch test on elastic and perfectly plastic materials with the three-dimensional finite element modeling, Wear 249 (2001) 422–432, http://dx.doi.org/10.1016/S0043-1648(01)00538-5.